


Global Analysis of Meningitis Disease With Optimal Control

Kwame Kyei Danquah¹, Sampson Takyi Appiah¹, Baaba A. Danquah¹,
Bernard Asamoah Afful^{2,*} , Godfred Agyemang Safo³

¹*Department of Mathematics and Statistics, University of Energy and Natural Resources, Ghana*
afriyiedanquah1@gmail.com, sampson.appiah@uenr.edu.gh, baaba.ghansah@uenr.edu.gh

²*Department of Mathematics and Statistics, Utah State University, Logan, UT, USA*
bernard.afful@usu.edu

³*English International School of Bratislava, Radničné námestie 4, Bratislava, Slovakia*
wisegas98@gmail.com

*Correspondence: *bernard.afful@usu.edu*

ABSTRACT. The meningitis epidemic has impacted lives negatively, especially in Sub-Saharan Africa, dubbed the 'Meningitis Belt'. The epidemic has been a public health concern due to an improper understanding of the disease's dynamics. To implement a control measure that will help minimize the epidemic, we introduce a non-linear Meningitis model that describes the dynamic behaviour of the disease and explains the transmission trend. The model explores the condition that leads to local or global asymptomatic stability of the equilibria. The model is subjected to a sensitivity analysis to find the parameters that influence the \mathcal{R}_0 . The model is modified into an optimal control by adding time-dependent controls. The control model is solved qualitatively using Pontryagin's maximum principle and numerically using MATLAB and the fourth-order Runge-Kutta method. We provide a control strategy that can be relied on for management decision-making based on the results.

1. INTRODUCTION

Meningitis, a deadly bacterial infection, is primarily attributed to Meningococcal meningitis. Meningitis kills over 100,000 individuals each year and affects 1.2 million people from all over the world. In Africa, especially the Sub-Saharan Africa meningitis belt, which extends from Senegal to Ethiopia, 10,000 people are expected to die each year [2]. This disease is widespread across sub-Saharan Africa, stretching from the meningitis belt in Senegal to Ethiopia. The illness reappears at the start of each dry season and disappears at the start of the rainy season in Africa, a fascinating pattern that warrants further study. Moreover, from the year 2003 to 2007, about 4100 cases of cerebrospinal Spinal Meningitis(CSM) were confirmed in the United States (CDC, 2017) [3]. It is approximated that during most significant epidemics, over 1000 cases of the disease are

Received: 10 Jun 2024.

Key words and phrases. Meningitis Disease; Optimal control; Global stability; Local stability; Sensitivity analysis.

reported, typically happening every 5 to 12 years [4]. The bacteria is transmitted from infected individuals to susceptible ones through contact with respiratory and throat secretions like saliva and mucus. However, unlike flu and common cold viruses, the bacteria are not highly contagious, and it takes time before transmission occurs. Those at risk of contracting the disease are typically individuals near the infected person, such as household members and roommates [5]. The most common signs of the disease include fever, headache and stiffness of the neck. Diagnosing the disease is sometimes difficult since the symptoms are often similar to other diseases [6]. Currently, a vaccine for meningitis exists, with the available vaccine primarily for bacteria such as meningitis. Bacterial meningitis is fatal when not diagnosed early [17]. Generally, infected individuals recover with permanent disabilities such as hearing loss and brain damage. These disabilities and the disease itself are worsened when symptoms are not detected on time.

Meningitis, a bacterial illness, has been a global concern, affecting numerous parts of the world. The disease has been endemic in several areas, with Sub-Saharan Africa being the hardest hit. Since its emergence, numerous models have been developed to describe the disease's transmission patterns, yet there remains a need for further understanding of intervention strategies to curb the disease in the Meningitis belt. In [15], and [16], the dynamical behaviour of the Meningitis disease was studied; however, the study failed to provide enough intervention and treatment strategies to minimize the disease. Against this background, we propose a non-linear mathematical Meningitis model that would analyse the model's stability and characterize a range of feasible control strategies that would aid management decision-making to curb the disease. In [31], the transmission behaviour of a meningitis disease is disclosed using an age-structured model that impacts the carriers' input to the model dynamics. The transmission behaviour of a Meningitis disease is revealed by building an age-structured model that affects the carriers' contribution to the model dynamics. [32] formulated a compartmental meningitis model that predicted the behavioural pattern of individuals and the population evolution by studying the dynamic trend of disease transmission. In their study, [33] studied the risk factor of Meningitis in adults by employing fuzzy cognitive maps and multi-criteria techniques to determine the ranks of the various scenarios. [34], determined the numerical solution of the Meningitis disease by considering the methods of Euler, Heun, and the fourth-order Runge-Kutta. In [35], the authors created a mathematical model to investigate the impact of shared information on the dynamics of Meningitis disease. The authors in [36] modelled a co-infection mathematical model of Listeriosis and Meningitis to unveil the parameters that impact the dynamics of the co-infection model. In [37], the authors formulated a mathematical model of influenza-meningitis co-infection that analysed the infected's outcome on the model's dynamics. In the paper by [39], the authors looked at a mathematical model of meningitis that attempted to explain the infection dynamics of the disease in Jirapa District, Ghana. To better understand the disease's transmission mechanisms, the researchers in [38] developed a mathematical meningitis model. The

model was subjected to a thorough stability study, with disease-free equilibrium indicating stability when $\mathcal{R}_0 \leq 1$ and endemic stability when $\mathcal{R}_0 \geq 1$.

Optimal controls are extensively used in dynamical systems, specifically those related to non-linear ordinary differential equations, and perceived as an intervention technique within control theory [40–43]. Mathematical models that involve optimal control analysis are essential for understanding disease spread and play a vital role in the policy-making process concerning disease control. The authors in [44] suggested a nonlinear mathematical model to see if public awareness campaigns affect the spread of infectious diseases. The model evaluated the population's response to media awareness because diseases spread through interaction between infected and susceptible people. Thus, the ability of the susceptible individuals to avoid contact with the infectives. Their analysis showed that infectious disease spread can be controlled by employing an awareness program. However, due to human immigration, diseases will always remain endemic. In [44], the authors explored the impact of media coverage on controlling disease spread by formulating a mathematical model incorporating media coverage. The analysis indicates that, even though the existence of media was not the sole factor in the attempt to eradicate the disease, its presence, to some extent, can minimize the number of infections. In [45], the authors attempted to reduce Ebola infection in the susceptible by constructing an optimal control theory from ordinary differential equation modelling of the Ebola virus. Two control functions, education and treatments, were considered in modelling the control problem. The control system is solved by applying the tool of Pontryagin's maximum principle. The analysis of the numerical results showed the controls' overall effect in reducing the disease. Also, the authors in [16] constructed a mathematical model of syphilis transmission dynamics to aid in selecting the most effective syphilis screening choices. The model created was an agent-based dynamic model that simulated a critical population of 2,000 people. According to the model's results, increasing the frequency of syphilis screening to every three months was very effective in reducing syphilis infection cases. In [46], the authors developed a mathematical model of COVID-19. To characterize a range of feasible controls that might be effective in minimizing the disease, the model was changed to an optimal control problem. A numerical simulation of the problem was performed using a forward-backwards sweep and fourth-order Runge-Kutta method. In [47], the authors created a mathematical model for the ongoing coronavirus outbreak to determine intervention approaches to battle it. The model was turned into an optimal control problem to provide a theoretical explanation for the disease, which was solved qualitatively by utilizing Pontryagin's maximal principle. MATLAB and an iterative technique were used to solve the models numerically.

The objective of this work is to design a mathematical model to investigate meningitis transmission, to examine the equilibrium's local and global stability, to conduct a sensitivity analysis of the

model parameters to identify the parameters that significantly affect the \mathcal{R}_0 , to formulate a control model for the Meningitis disease, and to perform a numerical simulation for the model.

The rest of the research is divided into the following sections: Section 2 focuses on formulating a nonlinear model for Meningitis disease. Section 3 explores the qualitative properties of the model, like positivity, solutions' boundedness, basic reproduction numbers, and the existence of equilibrium along with the local and global stability of disease-free and endemic equilibria. Section 4 centres on examining the sensitivity of the model's parameters on \mathcal{R}_0 using the normalized forward sensitivity index. In Section 5, the model is modified by adding time-dependent and solved with Pontryagin's Maximum Principle. Section 6 tackles computational investigations of the optimal control model based on the three control strategies, and the results are illustrated. Then, finally, we provide conclusions and discussions of the work in Section 7.

2. MATHEMATICAL MODEL

In the current section, a deterministic model for Meningitis disease that partitions the total population into S_{Hh} , susceptible, E_{Hh} , exposed, A_{Hh} , asymptomatic, I_{Hh} , symptomatic, and R_{Hh} , recovered is formulated. The population N is given as $N = S_{Hh} + E_{Hh} + A_{Hh} + I_{Hh} + R_{Hh}$. The model assumes that people are recruited into the population by birth at the rate Λ . The susceptible become exposed through contact with the symptomatic at rate η_1 . The exposed leaves at a rate τ_1 and enters the symptomatic while a fraction k_1 enters the asymptomatic. The asymptomatic and symptomatic die at rates τ_3 and ψ_2 , respectively. The asymptomatic can leave to recovery class due to natural immunity at rate τ_2 . The symptomatic enters the recovered compartments at a rate ψ_1 . The recovered individuals could return to the susceptible class due to loss of immunity at rate ω . With all the compartments, natural death occurs at a rate μ .

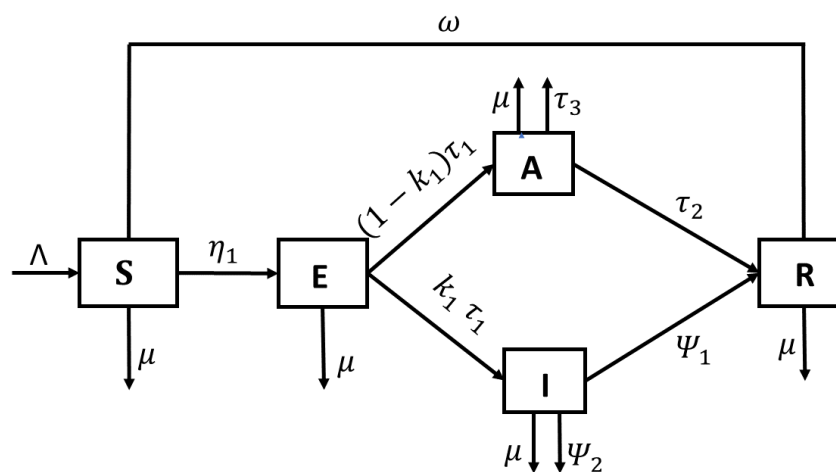


FIGURE 1. Schematic of the Meningitis model

$$\begin{aligned}
\frac{d}{dt}S_{Hh} &= \Lambda - \mu S_{Hh} - \eta_1 I_{Hh} S_{Hh} + \omega R_{Hh}, \\
\frac{d}{dt}E_{Hh} &= \eta_1 I_{Hh} S_{Hh} - k_1 \tau_1 E_{Hh} - (1 - k_1) \tau_1 E_{Hh} - \mu E_{Hh}, \\
\frac{d}{dt}A_{Hh} &= (1 - k_1) \tau_1 E_{Hh} - (\tau_2 + \tau_3 + \mu) A_{Hh}, \\
\frac{d}{dt}I_{Hh} &= k_1 \tau_1 E_{Hh} - (\psi_1 + \psi_2 + \mu) I_{Hh}, \\
\frac{d}{dt}R_{Hh} &= \tau_2 A_{Hh} + \psi_1 E_{Hh} - (\omega + \mu) R_{Hh},
\end{aligned} \tag{1}$$

with:

$$S_{Hh_0} \geq 0, E_{Hh_0} \geq 0, A_{Hh_0} \geq 0, I_{Hh_0} \geq 0 \text{ and } R_{Hh_0} \geq 0. \tag{2}$$

3. QUALITATIVE PROPERTIES

3.1. Positivity and Boundedness.

Theorem 3.1. *The set $\{S_{Hh}, E_{Hh}, A_{Hh}, I_{Hh}, R_{Hh}\}$ being the solution of the state system (1) with parameters which are non-negatives is positive with the initial condition given by;*

$$\{S_{Hh_0} \geq 0, E_{Hh_0} \geq 0, A_{Hh_0} \geq 0, I_{Hh_0} \geq 0, R_{Hh_0} \geq 0\}.$$

Proof. By inspection, the third equation of model (1) can be structured into a first-order differential equation standard form as:

$$\frac{d}{dt}A_{Hh} + (\tau_2 + \tau_3 + \mu)A_{Hh} = (1 - k_1)\tau_1 E_{Hh}. \tag{3}$$

When equation (3) is solved with the integrating factor method, we get

$$A_{Hh}(t) = e^{-(\tau_2 + \tau_3 + \mu)t} \left[A_{Hh}(0) + (1 - k_1)\tau_1 \int_0^t E(s) e^{-(\tau_2 + \tau_3 + \mu)s} ds \right].$$

The same method, when applied to the fourth equation, gives

$$I_{Hh}(t) = e^{-(\psi_1 + \psi_2 + \mu)t} \left[I_{Hh}(0) + k_1 \tau_1 \int_0^t E(s) e^{-(\psi_1 + \psi_2 + \mu)s} ds \right].$$

Hence, we observe that $\frac{d}{dt}A_{Hh} \geq 0$ at t_0 , $\frac{d}{dt}I_{Hh} \geq 0$ at t_0 . Thus, we can generalise that the other state variables remain positive at $t = 0$. Hence, the state model system 1 is positively invariant in \mathbb{R}_+^5 . \square

Theorem 3.2. *The model equation (1) is bounded within the invariant region, $\vartheta \in \mathbb{R}_+^5$ given as;*

$$\vartheta = \{(S_{Hh}, E_{Hh}, A_{Hh}, I_{Hh}, R_{Hh}) \in \mathbb{R}_+^5, S_{Hh} + E_{Hh} + A_{Hh} + I_{Hh} + R_{Hh} \leq \Lambda - \mu N\}.$$

Proof. We add the respective compartments to prove the boundedness of model system (1). Thus, we get

$$\begin{aligned} N(t) &= \Lambda - \mu S_{Hh} - \tau_3 A_{Hh} - \mu A_{Hh} - \mu E_{Hh} - \psi_2 I_{Hh} - \mu I_{Hh} - \mu R_{Hh}, \\ \frac{dN(t)}{dt} &= \Lambda - \tau_3 A_{Hh} - \psi_2 I_{Hh} - \mu N. \end{aligned} \quad (4)$$

It follows that from equation (4), setting H to be a solution of (4), we have a unique initial value problem,

$$\begin{cases} \frac{d}{dt} H_1(t) = \Lambda - \mu H_1(t) & t \geq 0 \\ H_1(0) = N(0). \end{cases} \quad (5)$$

The solution of (5) gives;

$$H_1(t) = N(0)e^{-\mu t} + \frac{\Lambda}{\mu}(1 - e^{-\mu t}). \quad (6)$$

What happens next is that, from the comparison Theorem in [1], we notice that,

$$N(t) = N(0)e^{-\mu t} + \frac{\Lambda}{\mu}(1 - e^{-\mu t}). \quad (7)$$

Therefore, from equation (7) the state variables $(S_{Hh}, E_{Hh}, A_{Hh}, I_{Hh}, R_{Hh})$ has the possible solution set which bounded and the model equation (1) is invariant $\mathfrak{D} \in \mathbb{R}_+^5$. As a result, model (1) is mathematically well-posed and epidemiologically feasible. \square

3.2. Existence of Disease-free equilibrium (DFE) point. Model system (1) has a trivial point $(0, 0, 0, 0, 0)$, which is usually ignored in the model's analysis. The right-hand side of (1) is set to zero and solved, the disease-free equilibrium becomes

$$\mathcal{E}_0 = \left(\frac{\Lambda}{\mu}, 0, 0, 0, 0 \right). \quad (8)$$

3.3. Basic reproduction number. The basic reproduction number, \mathcal{R}_0 , is one of the things that modellers look for when it comes to infectious disease modelling. The basic reproduction number is sufficient for determining the condition of the disease. In a completely naive population, the basic reproduction number is defined as the number of persons one infected person may infect. It is denoted by \mathcal{R}_0 , and when $\mathcal{R}_0 > 1$, it means the disease will spread unless preventive strategies are cautiously enacted. However, when $\mathcal{R}_0 < 1$, the infection dies without strenuous effort. The derivation of \mathcal{R}_0 is important in modelling and can be derived by the method of [19]. The (9) is the formulae guaranteeing \mathcal{R}_0 derivation.

$$\mathcal{R}_0 = \rho(\mathcal{FV}^{-1}). \quad (9)$$

The ρ is considered as the largest entry in the derivation of the next generation matrix of $\mathcal{R}_0 = \rho(\mathcal{FV}^{-1})$, where \mathcal{F} is the coming infection into compartment i and v . Thus, the transfer of individuals out of compartment i by death. Technically, the \mathcal{R}_0 becomes the largest eigenvalue of the

matrix resulting from the partial derivative of (9). What happens next is the infected compartments of model (1) are given by

$$\begin{aligned}\frac{d}{dt}E_{Hh} &= \eta_1 I_{Hh} S_{Hh} - k_1 \tau_1 E_{Hh} - (1 - k_1) \tau_1 E_{Hh} - \mu E_{Hh}, \\ \frac{d}{dt}A_{Hh} &= (1 - k_1) \tau_1 E_{Hh} - (\tau_2 + \tau_3 + \mu) A_{Hh}, \\ \frac{d}{dt}I_{Hh} &= k_1 \tau_1 E_{Hh} - (\psi_1 + \psi_2 + \mu) I_{Hh}.\end{aligned}$$

We notice from the diseased compartment that,

$$\mathcal{F} = \begin{bmatrix} \eta_1 I_{Hh} S_{Hh} \\ 0 \\ 0 \end{bmatrix}, \text{ and } \mathcal{V} = \begin{bmatrix} k_1 \tau_1 E_{Hh} + (1 - k_1) \tau_1 E_{Hh} + \mu E_{Hh} \\ -(1 - k_1) \tau_1 E_{Hh} + (\tau_2 + \tau_3 + \mu) A_{Hh} \\ -k_1 \tau_1 E_{Hh} + (\psi_1 + \psi_2 + \mu) I_{Hh} \end{bmatrix}. \quad (10)$$

When F is evaluated at \mathcal{E}_0 , then $F_{\mathcal{E}_0}$ becomes;

$$F_{\mathcal{E}_0} = \begin{bmatrix} 0 & 0 & \frac{\eta_1 \lambda}{\mu} \\ 0 & 0 & 0 \\ 0 & 0 & 0 \end{bmatrix}. \quad (11)$$

Evaluate V at \mathcal{E}_0 , which gives;

$$V_{\mathcal{E}_0} = \begin{bmatrix} (k_1 \tau_1 + \mu + (1 - k_1) \tau_1) & 0 & 0 \\ -(1 - k_1) \tau_1 & (\tau_2 + \tau_3 + \mu) & 0 \\ -k_1 \tau_1 & 0 & (\psi_1 + \psi_2 + \mu) \end{bmatrix}. \quad (12)$$

The basic reproduction number of model system (1) is determined by using the method of [19], which gives;

$$\mathcal{R}_0 = \frac{\eta_1 \wedge k_1 \tau_1}{\mu(k_1 \tau_1 + \mu + (1 - k_1) \tau_1)(\psi_1 + \psi_2 + \mu)}. \quad (13)$$

3.4. Existence of an endemic equilibrium point (EEP). Endemic equilibrium exists when there is a presence of infection. The model (1) has a unique endemic equilibrium given by;

$$\mathcal{E}^* = (S_{Hh}^*, E_{Hh}^*, A_{Hh}^*, I_{Hh}^*, R_{Hh}^*), \quad (14)$$

where

$$\begin{aligned}
 S_{Hh}^* &= \frac{\Lambda + \omega R_{Hh}^*}{\mu + \eta_1 I_{Hh}^*}, \\
 E_{Hh}^* &= \frac{\eta_1 I_{Hh}^* S_{Hh}^*}{(\mu + \tau_1)}, \\
 A_{Hh}^* &= \frac{(1 - k_1)\tau_1 E_{Hh}^*}{(\tau_2 + \tau_3 + \mu)}, \\
 I_{Hh}^* &= \frac{k_1 \tau_1 E_{Hh}^*}{(\psi_1 + \psi_2 + \mu)}, \\
 R_{Hh}^* &= \frac{\tau_2 A_{Hh}^* + \psi_1 E_{Hh}^*}{(\omega + \mu)}.
 \end{aligned}$$

3.5. Stability of the disease-free equilibrium point. Here, the global and local stability analyses of the Meningitis model (1) at the disease-free equilibrium are studied. The geometrical approach of Lyapunov function theory by [20] would be used to prove that model (1) is globally asymptotically stable at the disease-free equilibrium. The results are provided as follows;

$$\mathcal{J} = \begin{bmatrix} -\mu - \eta_1 I_{Hh} & 0 & 0 & -\eta_1 S_{Hh} & \omega \\ \eta_1 I_{Hh} & -(k_1 \tau_1 + \mu + (1 - k_1)\tau_1) & 0 & \eta_1 S_{Hh} & 0 \\ 0 & (1 - k_1)\tau_1 & -(\tau_2 + \tau_3 + \mu) & 0 & 0 \\ 0 & k_1 \tau_1 & 0 & -(\psi_1 + \psi_2 + \mu) & 0 \\ 0 & 0 & \tau_2 & \psi_1 & -(\omega + \mu) \end{bmatrix}. \tag{15}$$

Evaluating the Jacobian in (15) at the \mathcal{E}_0 gives;

$$J = \begin{bmatrix} -\mu & 0 & 0 & -\eta_1 \frac{\lambda}{\mu} & \omega \\ 0 & -(k_1 \tau_1 + \mu + (1 - k_1)\tau_1) & 0 & \eta_1 \frac{\Lambda}{\mu} & 0 \\ 0 & (1 - k_1)\tau_1 & -(\tau_2 + \tau_3 + \mu) & 0 & 0 \\ 0 & k_1 \tau_1 & 0 & -(\psi_1 + \psi_2 + \mu) & 0 \\ 0 & 0 & \tau_2 & \psi_1 & -(\omega + \mu) \end{bmatrix}.$$

clearly, $\lambda_1 = -\mu$, $\lambda_2 = -(\omega + \mu)$, $\lambda_3 = -(\tau_2 + \tau_3 + \mu)$. The remaining matrix becomes;

$$\hat{\mathcal{J}} = \begin{bmatrix} -(k_1 \tau_1 + \mu + (1 - k_1)\tau_1) & \eta_1 \frac{\Lambda}{\mu} \\ k_1 \tau_1 & -(\psi_1 + \psi_2 + \mu) \end{bmatrix}.$$

The characteristic equation is given by

$$\lambda^2 + b_1 \lambda + b_2 = 0 \tag{16}$$

where

$$b_1 = (k_1\tau_1 + \mu + (1 - k_1)\tau_1 + (\psi_1 + \psi_2 + \mu)),$$

$$b_2 = (k_1\tau_1 + \mu + (1 - k_1)\tau_1)(\psi_1 + \psi_2 + \mu) - \frac{\Lambda}{\mu}\eta_1 k_1\tau_1,$$

then

$$\lambda_{3,4} = \frac{-(b_1) \pm \sqrt{T_1}}{2},$$

where $T_1 = b_1^2 - 4b_2$. If $\lambda_3 \leq 0$ and $\lambda_4 \leq 0$, then the disease free equilibrium is stable. Otherwise, it is unstable.

Theorem 3.3. *When $R_0 < 1$, the disease-free equilibrium \mathcal{E}_0 for the Meningitis model (1) is globally asymptotically stable in R_+^5 .*

Proof. We construct a Lyapunov function

$$\mathcal{L} = k_1 \left(\frac{\tau_1}{d_1 d_2} \right) E_{Hh} + \frac{1}{d_2} I_{Hh},$$

where $d_1 = (k_1\tau_1 + \mu + (1 - k_1)\tau_1)$ and $d_2 = (\psi_1 + \psi_2 + \mu)$. Taking the derivative of \mathcal{L} with respect to E_{Hh} and I_{Hh} gives;

$$\frac{d\mathcal{L}}{dt} = k_1 \left(\frac{\tau_1}{d_1 d_2} \right) \frac{d}{dt} E_{Hh} + \frac{1}{d_2} \frac{d}{dt} I_{Hh},$$

$$\frac{d\mathcal{L}}{dt} = k_1 \left(\frac{\tau_1}{d_1 d_2} \right) (\eta_1 I_{Hh} S_{Hh} - k_1 \tau_1 E_{Hh} - (1 - k_1) \tau_1 E_{Hh} - \mu E_{Hh}) + \frac{1}{d_2} (k_1 \tau_1 E_{Hh} - (\psi_1 + \psi_2 + \mu) I_{Hh}),$$

$$\frac{d\mathcal{L}}{dt} = k_1 \left(\frac{\tau_1}{d_1 d_2} \right) (\eta_1 I_{Hh} S_{Hh} - d_1 E_{Hh}) + \frac{1}{d_2} (k \tau_1 E_{Hh} - d_2 I_{Hh}).$$

It follows that $S_{Hh} = \frac{\Lambda}{\mu}$ at t_0 . Hence

$$\begin{aligned} \frac{d\mathcal{L}}{dt} &= k_1 \left(\frac{\tau_1 \Lambda}{d_1 d_2 \mu} \right) \eta_1 I_{Hh} - \frac{k_1 \tau_1}{d_2} E_{Hh} + \frac{k_1 \tau_1}{d_2} E_{Hh} - I_{Hh}, \\ &= (\mathcal{R}_0 - 1) I_{Hh}. \end{aligned}$$

From the model equation (1), the system variables and parameters are all non-negative, implying that $\frac{d\mathcal{L}}{dt} < 0$ when $R_0 < 1$, with $\frac{d\mathcal{L}}{dt} = 0$ in the disease-free equilibrium. Hence, \mathcal{L} is a Lyapunov function in ψ . Hence, from [20] principle, $(E_{Hh}(t), I_{Hh}(t)) \rightarrow (0, 0)$ as $t \rightarrow \infty$. \square

3.6. Stability of the endemic equilibrium point. Here, we study the global and local stability of the Meningitis model (1) at the endemic equilibrium. The Lyapunov function method by [21] is employed to prove the globally asymptotic stability of model (1) at endemic equilibrium. The

underlying steps are, therefore, followed. The Jacobian evaluated at \mathcal{E}^* gives;

$$J = \begin{bmatrix} -\mu - \eta_1 l_{Hh}^* & 0 & 0 & -\eta_1 S_{Hh}^* & \omega \\ \eta_1 l_{Hh}^* & -(k_1 \tau_1 + \mu + (1 - k_1) \tau_1) & 0 & \eta_1 S_{Hh}^* & 0 \\ 0 & (1 - k_1) \tau_1 & -(\tau_2 + \tau_3 + \mu) & 0 & 0 \\ 0 & k_1 \tau_1 & 0 & -(\psi_1 + \psi_2 + \mu) & 0 \\ 0 & 0 & \tau_2 & \psi_1 & -(\omega + \mu) \end{bmatrix} \quad (17)$$

We denote $a = -\mu - \eta_1 l_{Hh}^*$, $b = -\eta_1 S_{Hh}^*$, $c = \omega$, $d = \eta_1 l_{Hh}^*$, $e = -(k_1 \tau_1 + \mu + (1 - k_1) \tau_1)$, $f = \eta_1 S_{Hh}^*$, $g = (1 - k_1) \tau_1$, $h = -(\tau_2 + \tau_3 + \mu)$, $i = k_1 \tau_1$, $j = -(\psi_1 + \psi_2 + \mu)$, $k = \tau_2$, $l = \psi_1$, and $m = -(\omega + \mu)$. Then, the characteristics equation of model (1) is given by

$$Y^5 + A_0 Y^4 + A_1 Y^3 + A_2 Y^2 + A_3 Y + A_4 = 0 \quad (18)$$

with

$$A_0 = (a + e + h + j + m),$$

$$A_1 = ae + ah + aj + eh + am + ej + -fi + em + hj + hm + jm,$$

$$A_2 = aeh + bdi + aej - afi + aem + ahj + ahm + ehj - fhi + ajm + ehm + ejm - fim + hjm,$$

$$A_3 = ehjm - fhim + bdhi + aehj - afhi - cdgk + aehm + bdim - cdil + aejm - afim + ahjm,$$

$$A_4 = -cdgjk + bdhim - cdhil + aehjm - afhim.$$

Based on the Routh-Hurwitz stability by [22], the condition for the characteristics equation (18) is given by

$$Y_i = \begin{bmatrix} Y_1 & Y_3 & Y_5 \\ Y_0 & Y_2 & Y_4 \\ 0 & Y_1 & Y_3 \\ 0 & Y_0 & Y_2 \\ 0 & 0 & Y_1 \\ 0 & 0 & Y_0 \\ 0 & 0 & 0 \end{bmatrix} > 0.$$

The condition requires all the coefficients of the characteristics equation (18) to be positive, implying that all eigenvalues have negative real parts. If the condition Y_i is satisfied, we conclude that the Meningitis model at the endemic equilibrium is stable and otherwise unstable.

Theorem 3.4. *When $R_0 \geq 1$, the endemic equilibrium \mathcal{E}^* of model 1 is stable when $S_{Hh} = S_{Hh}^*$, $E_{Hh} = E_{Hh}^*$, $A_{Hh} = A_{Hh}^*$, $I_{Hh} = I_{Hh}^*$, and $R_{Hh} = R_{Hh}^*$, otherwise unstable.*

Proof. We construct a Lyapunov function

$$\begin{aligned} \mathcal{L}_p = & \left(S_{Hh} - S_{Hh}^* - S_{Hh}^* \ln \left(\frac{S_{Hh}}{S_{Hh}^*} \right) \right) + \left(E_{Hh} - E_{Hh}^* - E_{Hh}^* \ln \left(\frac{E_{Hh}}{E_{Hh}^*} \right) \right) \\ & + \left(A_{Hh} - A_{Hh}^* - A_{Hh}^* \ln \left(\frac{A_{Hh}}{A_{Hh}^*} \right) \right) + \left(I_{Hh} - I_{Hh}^* - I_{Hh}^* \ln \left(\frac{I_{Hh}}{I_{Hh}^*} \right) \right) \\ & + \left(R_{Hh} - R_{Hh}^* - R_{Hh}^* \ln \left(\frac{R_{Hh}}{R_{Hh}^*} \right) \right). \end{aligned}$$

The derivative of \mathcal{L}_p with respect to t gives;

$$\begin{aligned} \frac{d\mathcal{L}_p}{dt} = & \left(\frac{S_{Hh} - S_{Hh}^*}{S_{Hh}} \right) \frac{dS_{Hh}}{dt} + \left(\frac{E_{Hh} - E_{Hh}^*}{E_{Hh}} \right) \frac{dE_{Hh}}{dt} + \left(\frac{A_{Hh} - A_{Hh}^*}{A_{Hh}} \right) \frac{dA_{Hh}}{dt} \\ & + \left(\frac{I_{Hh} - I_{Hh}^*}{I_{Hh}} \right) \frac{dI_{Hh}}{dt} + \left(\frac{R_{Hh} - R_{Hh}^*}{R_{Hh}} \right) \frac{dR_{Hh}}{dt}. \end{aligned} \quad (19)$$

Hence, substituting $\frac{dS_{Hh}}{dt}$, $\frac{dE_{Hh}}{dt}$, $\frac{dA_{Hh}}{dt}$, $\frac{dI_{Hh}}{dt}$ and $\frac{dR_{Hh}}{dt}$ into equation (19) gives;

$$\begin{aligned} \frac{d\mathcal{L}_p}{dt} = & \left(\frac{S_{Hh} - S_{Hh}^*}{S_{Hh}} \right) (\Lambda - \mu S_{Hh} - \eta_1 I_{Hh} S_{Hh} + \omega R_{Hh}) \\ & + \left(\frac{E_{Hh} - E_{Hh}^*}{E_{Hh}} \right) (\eta_1 I_{Hh} S_{Hh} - k\tau_1 E_{Hh} - (1 - k_1)\tau_1 E_{Hh} - \mu E_{Hh}) \\ & + \left(\frac{A_{Hh} - A_{Hh}^*}{A_{Hh}} \right) ((1 - k_1)\tau_1 E_{Hh} - (\tau_2 + \tau_3 + \mu)A_{Hh}) \\ & + \left(\frac{I_{Hh} - I_{Hh}^*}{I_{Hh}} \right) (k\tau_1 E_{Hh} - (\psi_1 + \psi_2 + \mu)I_{Hh}) \\ & + \left(\frac{R_{Hh} - R_{Hh}^*}{R_{Hh}} \right) (\tau_2 A_{Hh} + \psi_1 E_{Hh} - (\omega + \mu)R_{Hh}). \end{aligned}$$

Hence, for $S_{Hh} = S_{Hh}^*$, $E_{Hh} = E_{Hh}^*$, $A_{Hh} = A_{Hh}^*$, $I_{Hh} = I_{Hh}^*$, and $R_{Hh} = R_{Hh}^*$. We have that,

$$\begin{aligned} \frac{d\mathcal{L}_p}{dt} = & \Lambda - \Lambda \left(\frac{S_{Hh}^*}{S_{Hh}} \right) - \mu \left(\frac{(S_{Hh} - S_{Hh}^*)^2}{S_{Hh}} \right) - \eta_1 (I_{Hh} - I_{Hh}^*) \left(\frac{(S_{Hh} - S_{Hh}^*)^2}{S_{Hh}} \right) \\ & + \omega (R_{Hh} - R_{Hh}^*) \left(\frac{S_{Hh} - S_{Hh}^*}{S_{Hh}} \right) + \eta_1 \left(\frac{E_{Hh} - E_{Hh}^*}{E_{Hh}} \right) (I_{Hh} - I_{Hh}^*) (S_{Hh} - S_{Hh}^*) \\ & - k\tau_1 \left(\frac{(E_{Hh} - E_{Hh}^*)^2}{E_{Hh}} \right) - (1 - k_1)\tau_1 \left(\frac{(E_{Hh} - E_{Hh}^*)^2}{E_{Hh}} \right) - \mu \left(\frac{(E_{Hh} - E_{Hh}^*)^2}{E_{Hh}} \right) \end{aligned}$$

$$\begin{aligned}
& + (1 - k_1)\tau_1(E_{Hh} - E_{Hh}^*) \left(\frac{A_{Hh} - A_{Hh}^*}{A_{Hh}} \right) - (\tau_2 + \tau_3 + \mu) \left(\frac{(A_{Hh} - A_{Hh}^*)^2}{A_{Hh}} \right) \\
& + k\tau_1(E_{Hh} - E_{Hh}^*) \left(\frac{I_{Hh} - I_{Hh}^*}{I_{Hh}} \right) - (\psi_1 + \psi_2 + \mu) \left(\frac{(I_{Hh} - I_{Hh}^*)^2}{I_{Hh}} \right) \\
& + \tau_2(A_{Hh} - A_{Hh}^*) \left(\frac{R_{Hh} - R_{Hh}^*}{R_{Hh}} \right) + \psi_1(E_{Hh} - E_{Hh}^*) \left(\frac{R_{Hh} - R_{Hh}^*}{R_{Hh}} \right) \\
& - (\omega + \mu) \left(\frac{(R_{Hh} - R_{Hh}^*)^2}{R_{Hh}} \right).
\end{aligned}$$

We generate the below equation after thorough algebraic manipulations;

$$\frac{d\mathcal{L}_p}{dt} = \mathcal{G}_1 - \mathcal{G}_2, \quad (20)$$

where

$$\begin{aligned}
\mathcal{G}_1 = & \Lambda + \omega(R_{Hh} - R_{Hh}^*) \left(\frac{S_{Hh} - S_{Hh}^*}{S_{Hh}} \right) + \eta_1 \left(\frac{E_{Hh} - E_{Hh}^*}{E_{Hh}} \right) (I_{Hh} - I_{Hh}^*)(S_{Hh} - S_{Hh}^*) \\
& + (1 - k_1)\tau_1(E_{Hh} - E_{Hh}^*) \left(\frac{A_{Hh} - A_{Hh}^*}{A_{Hh}} \right) + k\tau_1(E_{Hh} - E_{Hh}^*) \left(\frac{I_{Hh} - I_{Hh}^*}{I_{Hh}} \right) \\
& + \tau_2(A_{Hh} - A_{Hh}^*) \left(\frac{R_{Hh} - R_{Hh}^*}{R_{Hh}} \right),
\end{aligned}$$

and

$$\begin{aligned}
\mathcal{G}_2 = & \Lambda \left(\frac{S_{Hh}^*}{S_{Hh}} \right) + \mu \left(\frac{(S_{Hh} - S_{Hh}^*)^2}{S_{Hh}} \right) + \eta_1(I_{Hh} - I_{Hh}^*) \left(\frac{(S_{Hh} - S_{Hh}^*)^2}{S_{Hh}} \right) \\
& + k\tau_1 \left(\frac{(E_{Hh} - E_{Hh}^*)^2}{E_{Hh}} \right) \mu \left(\frac{(E_{Hh} - E_{Hh}^*)^2}{E_{Hh}} \right) + (\tau_2 + \tau_3 + \mu) \left(\frac{(A_{Hh} - A_{Hh}^*)^2}{A_{Hh}} \right) \\
& + (\psi_1 + \psi_2 + \mu) \left(\frac{(I_{Hh} - I_{Hh}^*)^2}{I_{Hh}} \right) + (\omega + \mu) \left(\frac{(R_{Hh} - R_{Hh}^*)^2}{R_{Hh}} \right).
\end{aligned}$$

Hence, $\frac{d\mathcal{L}_p}{dt} = 0$ when $S_{Hh} = S_{Hh}^*$, $E_{Hh} = E_{Hh}^*$, $A_{Hh} = A_{Hh}^*$, $I_{Hh} = I_{Hh}^*$, and $R_{Hh} = R_{Hh}^*$. It can be shown that the inequality $\mathcal{G}_1 \leq \mathcal{G}_2$. Evidently, it can be verified that $\frac{d\mathcal{L}_p}{dt} \leq 0$ when $\mathcal{G}_1 \leq \mathcal{G}_2$. Hence $\frac{d\mathcal{L}_p}{dt} = 0$, when $S_{Hh} = S_{Hh}^*$, $E_{Hh} = E_{Hh}^*$, $A_{Hh} = A_{Hh}^*$, $I_{Hh} = I_{Hh}^*$ and $R_{Hh} = R_{Hh}^*$. This indicates that the largest compact invariant set is a Singleton. Hence, from [20], \mathcal{E}^* is globally stable. \square

4. SENSITIVITY ANALYSIS OF \mathcal{R}_0

Getting the correct estimation of the \mathcal{R}_0 in infection disease modelling is crucial because it helps us in the decisions concerning the management of the infection. However, the possibility of the parameters linked to the \mathcal{R}_0 to change makes sensitivity analysis an important subject in epidemiology.

Definition 4.1. *The normalized forward sensitivity index of \mathcal{R}_0 computed using the formula used by [23] for a given parameter α_1 is*

$$\vartheta_{\alpha_1}^{\mathcal{R}_0} = \frac{\partial \mathcal{R}_0}{\partial \alpha_1} \frac{\alpha_1}{\mathcal{R}_0}. \quad (21)$$

The parameters with positive indices contribute to the epidemic spreading since they enhance the \mathcal{R}_0 . The parameters with a negative index, on the other hand, aid in disease control by lowering \mathcal{R}_0 . From Table 1, Λ , τ_1 , ψ_1 , η_1 , k_1 , μ , and ψ_2 are the parameters which are most sensitive on \mathcal{R}_0 .

TABLE 1. Model Parameter Sensitivity Indices for the Reproduction Number

Parameter	Sensitivity Index
Λ	1.000
τ_1	-2.333
ψ_1	-0.526
ψ_2	-0.473
η_1	1.000
μ	-1.000
k_1	1.000

This is because, any increment in the parameter values of Λ , η_1 , and k_1 will lead to a 100% increase in \mathcal{R}_0 . Also, an increase in μ , τ_1 , ψ_1 , and ψ_2 , will decrease \mathcal{R}_0 by 100%, 233.3%, 52.6% and 47.3% respectively. Therefore, effective measures must be put in place to decrease Λ , η_1 , and k_1 and to increase μ , $\tau_1\psi_1$, and ψ_2 . Although intervention measures are geared towards increasing and/or increasing the most significant parameters, it is paramount that the control of the other parameters not be completely ignored.

5. OPTIMAL CONTROL ANALYSIS

In this section, model system (1) is modified by putting in three time-dependent controls, viz. personal protection, vaccination and treatment controls, to examine the impact of the control schemes on the Meningitis disease. In model system (1), the associated infection force is lowered by a factor of $(1 - u_1)$, where u_1 is the personal protection control that ensures the attempt to reduce room heat and avoid close contact with the infected. The rate of vaccinating susceptible individuals against Meningitis is represented by the control function u_2 . As a result, the model assumes that vaccinated individuals shift from the susceptible compartment to the removed compartment at any time. Furthermore, we assume that the control function u_3 reflects the rate at which sick patients

are treated. Hence, the modified nonlinear control system becomes;

$$\begin{aligned}
 \frac{dS_{Hh}}{dt} &= \Lambda - \mu S_{Hh} - (1 - u_1)\eta_1 I_{Hh} S_{Hh} + \omega R_{Hh} - u_2 S_{Hh}, \\
 \frac{dE_{Hh}}{dt} &= (1 - u_1)\eta_1 I_{Hh} S_{Hh} - k\tau_1 E_{Hh} - (1 - k_1)\tau_1 E_{Hh} - \mu E_{Hh}, \\
 \frac{dA_{Hh}}{dt} &= (1 - k_1)\tau_1 E_{Hh} - (\tau_2 + \tau_3 + \mu)A_{Hh}, \\
 \frac{dI_{Hh}}{dt} &= k\tau_1 E_{Hh} - (\psi_1 + \psi_2 + u_3 + \mu)I_{Hh}, \\
 \frac{dR_{Hh}}{dt} &= \tau_2 A_{Hh} + \psi_1 E_{Hh} + u_2 S_{Hh} + u_3 I_{Hh} - (\omega + \mu)R_{Hh}.
 \end{aligned} \tag{22}$$

To examine the efforts needed to control the disease, we define an optimal functional \mathcal{J} that minimizes the exposed, asymptomatic and symptomatic individuals and maximizes the recovery through personal protection, vaccination and treatment controls of u_1 , u_2 and u_3 . Hence, the objective functional \mathcal{J} is given by;

$$\mathcal{J}(u_1, u_2, u_3) = \int_0^{t_f} \left[B_1 E_{Hh} + B_2 A_{Hh} + B_3 I_{Hh} + \frac{1}{2}(u_1^2 d_1 + u_2^2 d_2 + u_3^2 d_3) \right] dt. \tag{23}$$

Referring to (23), the quantities B_1 , B_2 , and B_3 are the weight coefficients of the exposed, asymptomatic and symptomatic individuals. In addition, the terms $\frac{u_1^2 d_1}{2}$, $\frac{u_2^2 d_2}{2}$ and $\frac{u_3^2 d_3}{2}$ represents the cost related to minimizing the exposed, asymptomatic and symptomatic individual. The control model considers a quadratic cost on the controls as in other works. We target optimal control u_1^* , u_2^* , u_3^* such that

$$\mathcal{J}(u_1^*, u_2^*, u_3^*) = \min\{\mathcal{J}(u_1, u_2, u_3) : (u_1, u_2, u_3) \in \mathcal{U}\}, \tag{24}$$

where

$$\mathcal{U} = \{(u_1, u_2, u_3) | 0 \leq u_i \leq 1, i = 1, 2, 3 \text{ Lebesgue measurable}\} \tag{25}$$

With the method of Pontryagin's maximum principle [24], system (22) and (23) are transformed into a problem of Hamiltonian minimization \mathcal{H} with respect to the controls u_1 , u_2 and u_3 where;

$$\begin{aligned}
 \mathcal{H} &= \left[B_1 E_{Hh} + B_2 A_{Hh} + B_3 I_{Hh} + \frac{1}{2}(u_1^2 d_1 + u_2^2 d_2 + u_3^2 d_3) \right], \\
 &+ \lambda_1 \{ \Lambda - \mu S_{Hh} - (1 - u_1)\eta_1 I_{Hh} S_{Hh} + \omega R_{Hh} - u_2 S_{Hh} \}, \\
 &+ \lambda_2 \{ (1 - u_1)\eta_1 I_{Hh} S_{Hh} - k\tau_1 E_{Hh} - (1 - k_1)\tau_1 E_{Hh} - \mu E_{Hh} \}, \\
 &+ \lambda_3 \{ (1 - k_1)\tau_1 E_{Hh} - (\tau_2 + \tau_3 + \mu)A_{Hh} \}, \\
 &+ \lambda_4 \{ k\tau_1 E_{Hh} - (\psi_1 + \psi_2 + u_3 + \mu)I_{Hh} \}, \\
 &+ \lambda_5 \{ \tau_2 A_{Hh} + \psi_1 E_{Hh} + u_2 S_{Hh} + u_3 I_{Hh} - (\omega + \mu)R_{Hh} \}.
 \end{aligned} \tag{26}$$

Theorem 5.1. *There exists an optimal control $U^* = (u_1^*, u_2^*, u_3^*) \in \mathcal{U}$ such that*

$$\mathcal{J}(u_1^*, u_2^*, u_3^*) = \min_{U \in \mathcal{U}} \mathcal{J}(u_1, u_2, u_3), \quad (27)$$

subject to the control system 22 with the initial conditions.

Proof. The work of [25] would be considered the grounds for proving the existence of optimal control. In minimizing the control problem, the necessary and convexity of the objective functional in u_1 , u_2 and u_3 are satisfied. The control space \mathcal{U} is also convex and closed by definition.

The optimal control system is bounded, which verifies the compactness necessary for the optimal control. Also, the integrand in the functional (23) is convex on \mathcal{U} . Therefore, we notice that there exist a constant $q > 1$, positive numbers u_1 , u_2 and u_3 such that,

$$J(u_1, u_2, u_3) \geq u_1 (|u_1|^2 + |u_2|^2 + |u_3|^2)^{\frac{q}{2}} - u^2$$

□

Hence, there exists an optimal control. It follows that determining the optimal solution, the Pontryagin's maximum principle by [26] is applied to the Hamiltonian (26) such that given (y, u) is an optimal solution of the optimal control problem, then there exist a non-trivial vector function $\lambda = (\lambda_1, \dots, \lambda_5)$ satisfying the below equation;

$$\begin{aligned} \frac{dy}{dt} &= -\frac{\partial \mathcal{H}(t, y, u, \lambda)}{\partial \lambda}, \\ 0 &= \frac{\partial \mathcal{H}(t, y, u, \lambda)}{\partial u}, \\ \frac{d\lambda}{dt} &= \frac{\partial \mathcal{H}(t, y, u, \lambda)}{\partial y}. \end{aligned} \quad (28)$$

Hence, the necessary condition related to the Hamiltonian (26) is applied.

Theorem 5.2. *Given that S_{Hh}^* , E_{Hh}^* , A_{Hh} , I_{Hh}^* and R_{Hh}^* are optimal state solutions with associated optimal control variables (u_1^*, u_2^*, u_3^*) for the optimal control problem (22) and (23), then there exist adjoint variables λ_i for $i = 1, \dots, 5$, satisfying;*

$$\begin{aligned} \frac{d\lambda_1}{dt} &= (\lambda_1 - \lambda_2)(1 - u_1)\eta_1 I_{Hh} + (\lambda_2 - \lambda_5)u_2 + \mu\lambda_1, \\ \frac{d\lambda_2}{dt} &= -B_1 + (\lambda_2 - \lambda_3)(1 - k_1)\tau_1 + (\lambda_2 - \lambda_4)k\tau_1 + \mu\lambda_2, \\ \frac{d\lambda_3}{dt} &= -B_2 + (\tau_3 + \mu)\lambda_3 + (\lambda_3 - \lambda_5)\tau_2, \\ \frac{d\lambda_4}{dt} &= -B_3 + (\lambda_1 - \lambda_2)(1 - u_1)\eta_1 S_{Hh} + (\lambda_4 - \lambda_5)\psi_1 + (\psi_2 + \mu)\lambda_4 + (\lambda_4 - \lambda_5)u_3, \\ \frac{d\lambda_5}{dt} &= (\lambda_5 - \lambda_1)\omega + \mu\lambda_5, \end{aligned} \quad (29)$$

with boundary condition;

$$\lambda_i(t_f) = 0, \quad i = 1, 2, \dots, 5, \quad (30)$$

and the optimal control u_1^* , u_2^* and u_3^* are given by

$$\begin{cases} u_1^* = \min \left\{ 1, \max \left\{ 0, \left((\lambda_2 - \lambda_1) \frac{\eta_1 I_{Hh} S_{Hh}}{d_1} \right) \right\} \right\} \\ u_2^* = \min \left\{ 1, \max \left\{ 0, (\lambda_1 - \lambda_5) \frac{S_{Hh}}{d_2} \right\} \right\} \\ u_3^* = \min \left\{ 1, \max \left\{ 0, (\lambda_4 - \lambda_5) \frac{I_{Hh}}{d_3} \right\} \right\} \end{cases} \quad (31)$$

Proof. The adjoint and transversality conditions are derived using the Hamiltonian (26). Thus we equate $S_{Hh} = S_{Hh}^*$, $E_{Hh} = E_{Hh}^*$, $A_{Hh} = A_{Hh}^*$, $I_{Hh} = I_{Hh}^*$ and $R_{Hh} = R_{Hh}^*$ and differentiating the Hamiltonian with respect to S_{Hh} , E_{Hh} , A_{Hh} , I_{Hh} and R_{Hh} to obtain (29). Further, the equations

$$\frac{\partial \mathcal{H}}{\partial u_1} = 0, \quad \frac{\partial \mathcal{H}}{\partial u_2} = 0, \quad \frac{\partial \mathcal{H}}{\partial u_3} = 0. \quad (32)$$

are determined on the interior of the control set, and using the optimality conditions and the property of the control space u_1 and u_2 , we can determine (22). From (22), we can characterize the control found by solving the optimality system. In solving the optimality system, the transversality and the characterization of the optimal control (u_1, u_2, u_3) are used. The controls u_1^* , u_2^* and u_3^* when substituted into the control system (22) gives;

$$\begin{cases} \frac{dS_{Hh}}{dt} = \Lambda - \mu S_{Hh} - \left(1 - \min \left\{ 1, \max \left\{ 0, \left((\lambda_2 - \lambda_1) \frac{\eta_1 I_{Hh} S_{Hh}}{d_1} \right) \right\} \right\} \right) \eta_1 I_{Hh} S_{Hh} \\ \quad + \omega R_{Hh} - (\lambda_1 - \lambda_5) \frac{S_{Hh}}{d_2} S_{Hh}, \\ \frac{dE_{Hh}}{dt} = \left(1 - \min \left\{ 1, \max \left\{ 0, \left((\lambda_2 - \lambda_1) \frac{\eta_1 I_{Hh} S_{Hh}}{d_1} \right) \right\} \right\} \right) \eta_1 I_{Hh} S_{Hh} \\ \quad - k\tau_1 E_{Hh} - (1 - k_1)\tau_1 E_{Hh} - \mu E_{Hh}, \\ \frac{dA_{Hh}}{dt} = (1 - k_1)\tau_1 E_{Hh} - (\tau_2 + \tau_3 + \mu)A_{Hh}, \\ \frac{dI_{Hh}}{dt} = k\tau_1 E_{Hh} - \left(\psi_1 + \psi_2 + \min \left\{ 1, \max \left\{ 0, (\lambda_1 - \lambda_5) \frac{S_{Hh}}{d_2} \right\} \right\} + \mu \right) I_{Hh}, \\ \frac{dR_{Hh}}{dt} = \tau_2 A_{Hh} + \psi_1 E_{Hh} + \min \left\{ 1, \max \left\{ 0, (\lambda_1 - \lambda_5) \frac{S_{Hh}}{d_2} \right\} \right\} S_{Hh} \\ \quad + \min \left\{ 1, \max \left\{ 0, (\lambda_4 - \lambda_5) \frac{I_{Hh}}{d_3} \right\} \right\} I_{Hh} - (\omega + \mu)R_{Hh}. \end{cases} \quad (33)$$

□

6. NUMERICAL SIMULATION AND DISCUSSION

The present section focuses on obtaining a numerical solution for the model. Besides the qualitative analysis that has been carried out, it becomes imperative to find a numerical solution for the model. Hence, our task here is to derive a numerical solution that solves the without and with control models and evaluates the effectiveness of the considered control strategies. A numerical algorithm uses a 4th-order Runge-Kutta method and MATLAB to solve the optimality system. Thus, a numerical solution of the control optimality system involves running the adjoint system backwards

and the state forward in time, with the associated boundary conditions and the controls. The process involves continuously upgrading the controls and the characterization value until the earlier results become close to the currently obtained value; then, the algorithm stops, and a solution is obtained. The MATLAB simulation was done with values taken from the published work. Below are the parameters considered for the simulation.

TABLE 2. Meningitis Model Parameters

Parameter	Description	Range	Estimated Value	Reference
Λ	Recruitment rate	(100 – 100000)	1000	[3]
τ_1	Modification parameter	(0.001 – 0.8)	0.3	[3]
τ_2	Rate at individuals leaves the asymptomatic class	(0.002 – 0.3)	0.03	[3]
τ_3	Disease induced death rate	(0.002 – 0.2)	0.2	[3]
ψ_1	Rate at which individuals leave the infected class to the recovered class	(0.001 – 0.1)	0.02	[27]
ψ_2	Disease induced death rate	(0.002 – 0.1)	0.018	[3]
ω	Loss of immunity	(0.01 – 0.1)	0.084	[48]
η_1	Contact rate	(0.1 – 0.9)	0.5	[28]
μ	Rate at which individuals naturally leaves the compartment	(0.00001 – 0.2)	0.0000391	[29]
k_1	Rate at which individuals leaves the exposed class	(0.01 – 0.5)	0.3	[30]

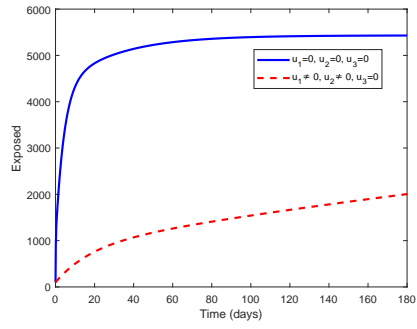
6.1. **Strategy A** : $u_3 = 0$. Strategy A uses the controls u_1 and u_2 , with u_3 set to zero. The graphs of 2a, 2b, 2c and 2d Indicate the exposed, asymptomatic, and symptomatic people, as well as the controls. The without-control graph of 2a showed a swift increase of an estimated 5000 in the first 20 days. Moreover, it remained at this level throughout the remaining simulated time. With the asymptomatic non-control graph of 2b, we notice a gentle rise of the graph in the first 20 days to 4300 of the asymptomatic population. The asymptomatic control graph progressed steadily to a new 5000 in 140 days and retained it till the end of the simulation. The symptomatic non-control graph of 2c increased smoothly and moved to the maximum height of 430 of the symptomatic population in 130 days, which remained until the end of the simulation. Control figures of the exposed, asymptomatic and symptomatic produced results with substantially minimized graphs. From the exposed graph of 2a, the graph increases similarly but could not rise to the level of the without

control plot. We see that the control graph has been dramatically minimized. The control figures 2b of the asymptomatic lie far below the non-control figure. The symptomatic control figure of 2c lay slightly above zero and maintained the level throughout the simulated time. Figure 2d is the control profile plot of strategy A. The plot shows that the personal protection procedure u_1 remained at the Upper bound throughout the simulation, while the vaccine control u_2 remained at the upper bound until 178 days before dropping to the lower bound.

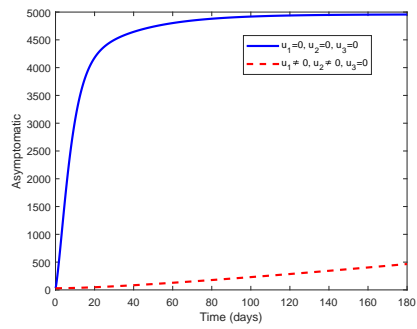
6.2. **Strategy B** : $u_2 = 0$. Strategy B sets $u_2 = 0$ and generates the exposed, asymptomatic, and symptomatic graphs. From the exposed graph of a , we observed that the without control curve swiftly raised to 5000 when $t = 20$. It moved gently to about 5100 for the next 20 days and remained at that level for the remaining time. The asymptomatic without control curve steadily increased in the early days of 20 to 4500, increased gently for the next 120 days to 5000, and maintained the level for the remaining time. The symptomatic without control graph increased smoothly and progressed to a height of 430 at the final time. The exposed, asymptomatic and symptomatic control graphs produced graphs with desired results. Thus, we noticed a completely minimized exposure, asymptomatic and symptomatic, with the control simulations. Figure 3d is the control profile graph. The graph shows that the personal protection and treatment controls remained at the upper bound until 100 and 98 when they dropped to the lower bound. The simulated plots of the exposed, asymptomatic and symptomatic confirmed that strategy B is effective.

6.3. **Strategy C** : $u_1 = 0$. Strategy C uses the control $u_1 = 0$ and the remaining controls for the simulated. The graphs of 4a, 4b, 4c, and 4d are the exposed, asymptomatic, symptomatic and control profile plots of strategy C. In the early days, the exposure surged swiftly for the without control graphs but maintained a stable level after 40 days. The asymptomatic graph moved steeply in the early days of 20 to 4500, increased further to 5000 for the next 120, and retained the level for the remaining days. The symptomatic graph gently increased throughout the simulation and maintained a steady progression. The exposed control plot showed a swift increase in the graph in the early days and progressed gently for the entire simulated time. The asymptomatic control graph smoothly increased in the early days and progressed with the same momentum for the rest of the simulation. The symptomatic control curve was noticed to be minimized throughout the entire simulation. The plot of figure 4d is the optimal control profile of strategy C. The vaccine (u_2) and treatment (u_3) controls remained at the upper bound throughout the simulation until 180 days, when they decreased to the lower bound.

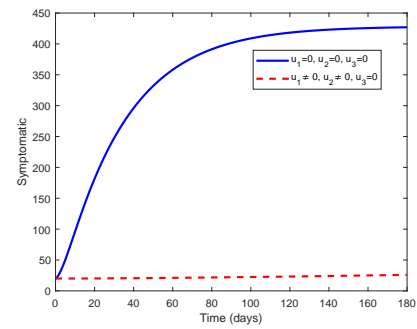
6.4. **Strategy D** : $u_1 \neq 0$, $u_2 \neq 0$ and $u_3 \neq 0$. Strategy D considered the three controls in its simulation and generated the exposed, asymptomatic and symptomatic plots. Without control, the exposed graph sparked to 2000 at $t = 0$. The graphs increased steadily to 5000 in 20 days and then retained it for the rest of the time. The asymptomatic graph also increased early in the first



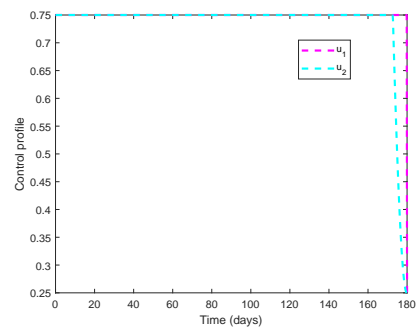
(A)



(B)

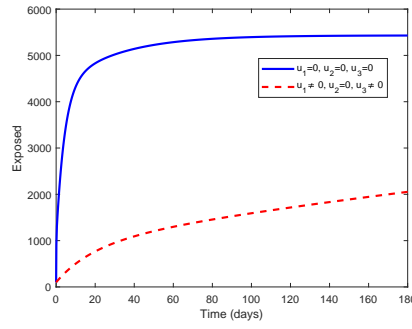


(C)

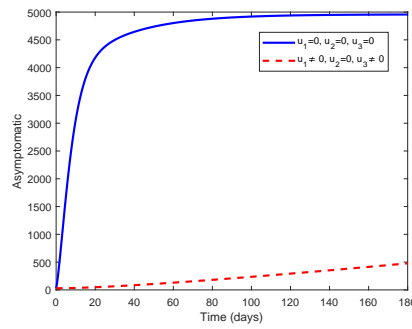


(D)

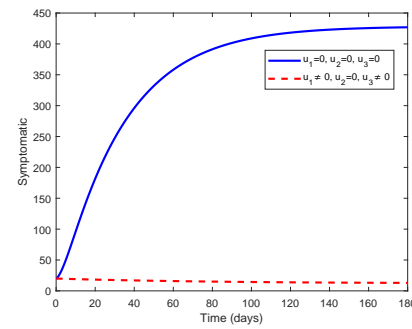
FIGURE 2. plot of phase portraits with $u_3 = 0$



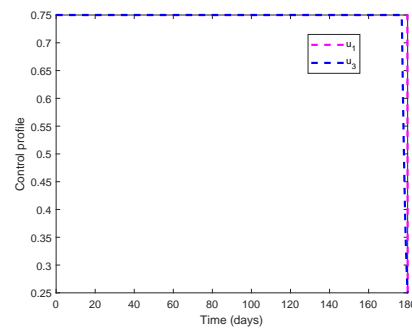
(A)



(B)

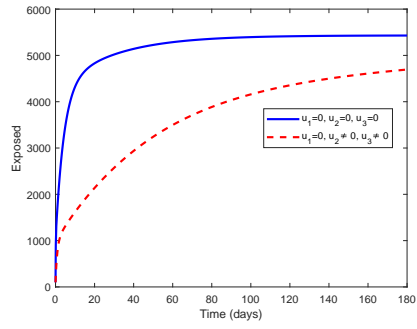


(C)

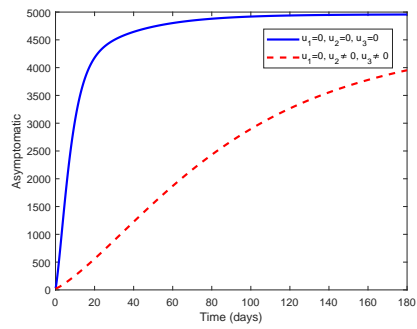


(D)

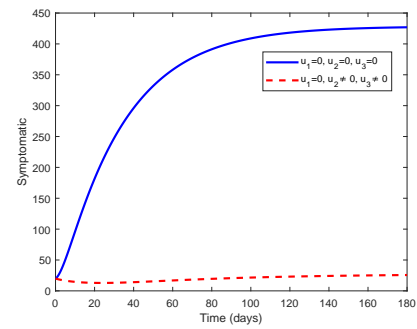
FIGURE 3. plot of phase portraits with $u_2 = 0$



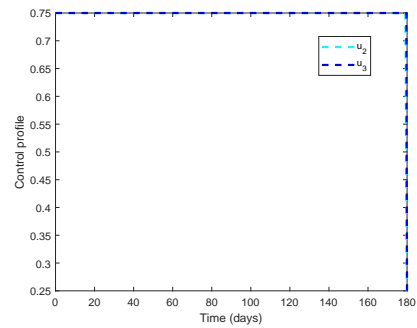
(A)



(B)



(C)



(D)

FIGURE 4. plot of phase portraits with $u_1 = 0$

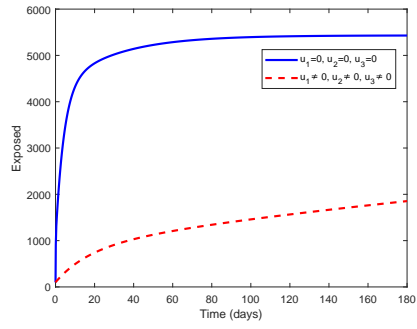
20 days to 4500 and then smoothly progressed to 5000 for the next 100 days and maintained the level. The symptomatic level gradually rose from 10 in a day (1) to 430 in 180 days. With the control application, witnessed the exposure raised 1000 to 1900 in 180 days. The asymptomatic slightly raised slightly below 500 for the 1180 days. The symptoms could barely move above 10. Plot 4d is the control profile plot of strategy D, We notice from the control plot that the personal protection, vaccination and treatment controls remained at the upper bound until 180, 178, and 177 respectively when they dropped to the lower bound.

7. DISCUSSION AND CONCLUSION

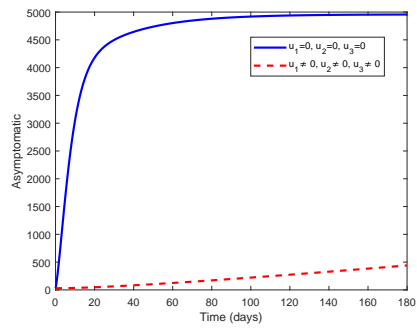
The study considered a non-linear compartmental model of meningitis disease to explain the transmission dynamics. The compartmental Meningitis model was presented, with compartments for Susceptible(S), Exposed(E), Asymptomatic(A), Symptomatic(I), and Recovered(R). The model's equilibria and the basic reproduction number were determined. The model's local stability at the two equilibrium points, the disease-free and endemic, was determined by using the linearisation approach. The global stabilities of the equilibria were investigated by employing the geometric method of the Lyapunov function. In addition, a sensitivity analysis was carried out on the \mathcal{R}_0 to determine the parameters that significantly affect the \mathcal{R}_0 . It was seen that the most sensitive parameters on \mathcal{R}_0 are Λ , τ_1 , ψ_1 , η_1 , k_1 , μ , and ψ_2 .

An optimal control model was formulated by adding time-dependent optimal controls. By defining time-dependent policies that might help decrease or eradicate the disease, the model was changed into an optimal control problem. To discover the optimality conditions of the systems, the control model was solved using Pontryagin's maximum principle. Several works have been done on meningitis transmission, but few have considered optimal control. As a result, we formulated the Meningitis model that was modified to optimal control problems to characterise a range of possible strategies to help control the disease. Therefore, we considered possible pairing of the controls to examine their combined effect on the disease.

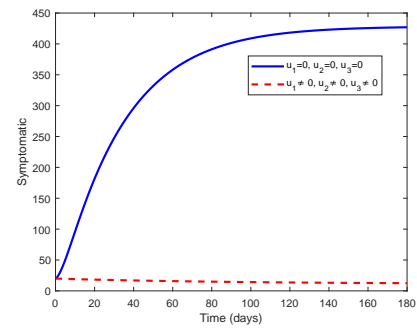
With strategy A, the controls of personal protection and vaccination were considered. The graphs of 2a, 2b, 2c, and 2d denote the exposed, asymptomatic and symptomatic individuals and the control profile. Without control, the graph of 2a showed a swift increase of an estimated 5000 in the first 20 days. Moreover, it remained at this level throughout the remaining simulated time. With the asymptomatic non-control graph of 2b, we notice a gentle rise of the graph in the first 20 days to 4300 of the asymptomatic population. The asymptomatic control graph progressed steadily to a new level of 5000 in 140 days and retained at that level till the end of the simulation. The symptomatic non-control graph of 2c increased smoothly and moved to the maximum height of 430 of the symptomatic population in 130 days, which remained until the end of the simulation. Control figures of the exposed, asymptomatic and symptomatic produced results with substantially minimized graphs. From the exposed graph of 2c, the graph increases similarly but could not rise



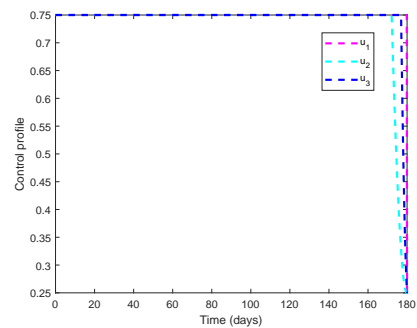
(A)



(B)



(C)



(D)

FIGURE 5. plot of phase portraits with $u_1 \neq 0, u_2 \neq 0$ and $u_3 \neq 0$

to the level of the without control plot. We see that the control graph has been dramatically minimized. The control figures 2b of the asymptomatic lies far below the non-control figure. The symptomatic control figure of 2d lay slightly above zero and maintained the level throughout the simulated time.

Strategy B considered personal protection and treatment control. From the exposed graph of 2a, we observed that the without control curve swiftly raised to 5000 when $t = 20$. It moved gently to about 5100 for the next 20 days and remained at that level for the remaining time. The asymptomatic without control curve steadily increased in the early days of 20 to 4500, increased gently for the next 120 days to 5000, and maintained the level for the remaining time. The symptomatic without control graph increased smoothly and progressed to a height of 430 at the final time. The exposed, asymptomatic and symptomatic control graphs produced graphs with desired results. Thus, we noticed a completely minimized exposure, asymptomatic and symptomatic, with the control simulations.

Strategy C paired the vaccination and treatment controls. We noticed that the exposure surged swiftly for the graphs without control in the early days but maintained a stable level after 40 days. The asymptomatic graph moved steeply in the early days of 20 to 4500, increased further to 5000 for the next 120, and retained it for the remaining days. The symptomatic graph gently increased throughout the simulation and maintained a steady progression. The exposed control plot showed a swift increase in the graph in the early days and progressed gently for the entire simulated time. The asymptomatic control graph climbed gradually in the early days and continued throughout the simulation. Throughout the simulation, the symptomatic control curve was found to be minimized.

Strategy D paired all three controls. Without control, the exposed graph rose to 2000 at $t = 0$. The graphs increased steadily to 5000 in day 20 and then maintained that level for the rest of the time. The asymptomatic graph also increased early in the first 20 days to 4500 and then smoothly progressed to 5000 for the next 100 days and retained the level. The symptomatic level gradually rose from 10 in a day (1) to 430 in 180 days. With the control application, we witnessed the exposed raised 1000 to 1900 in 180 days. The asymptomatic slightly raised slightly below 500 for the 1180 days. The symptomatic could not move above 10. The simulated results showed that the strategies significantly minimise the disease. It can be concluded that the combination of the three controls or two controls can be employed when it comes to meningitis control. A cost-benefit analysis of the combinations shown needs to be performed.

REFERENCES

- [1] J. K. K. Asamoah, M.A. Owusu, Z. Jin, F.T. Oduro, A. Abidemi, E.O. Gyasi, Global stability and cost-effectiveness analysis of covid-19 considering the impact of the environment: using data from Ghana, *Chaos Solitons Fractals* 140 (2020), 110103.

- [2] D. A. Caugant, Population genetics and molecular epidemiology of *Neisseria meningitidis*, *APMIS*. 106 (1998), 505–525.
- [3] J. K. K. Asamoah, F. Nyabadza, B. Seidu, M. Chand, H. Dutta, Mathematical modelling of bacterial meningitis transmission dynamics with control measures, *Comp. Math. Meth. Med.* 2018 (2018), 2657461.
- [4] F. M. LaForce, J. M. Okwo-Bele, Eliminating epidemic Group A meningococcal meningitis in Africa through a new vaccine. *Health affairs (Project Hope)*, 30 (2011), 1049–1057.
- [5] B. Sultan, K. Labadi, J. F. Guégan, S. Janicot, Climate drives the meningitis epidemics onset in west Africa, *PLoS Med.* 2 (2005), e6.
- [6] F. Y. Aku, F. C. Lessa, F. Asiedu-Bekoe, P. Balagumyetime, W. Ofofu, J. Farrar, et al. Meningitis Outbreak Caused by Vaccine-Preventable Bacterial Pathogens - Northern Ghana, 2016. *MMWR. Morb. Mort. Weekly Rep.* 66 (2017), 806–810.
- [7] E. J. C. Goldstein, R. H. Johnson, H. E. Einstein, Coccidioidal Meningitis. *Clinical Infectious Diseases*, 42 (2006), 103–107.
- [8] R. D. Feigin, G. H. McCracken, Jr, J. O. Klein, Diagnosis and management of meningitis, *Pediatric Infect. Dis. J.* 11 (1992), 785–814.
- [9] D. Swanson, Meningitis, *Pediatr. Rev.* 36 (2015), 514–526.
- [10] A. Schuchat, K. Robinson, J. D. Wenger, L.H. Harrison, M. Farley, A. L. Reingold, L. Lefkowitz, B. A. Perkins, Bacterial meningitis in the united states in 1995, *N. Engl. J. Med.* 337 (1997), 970–976. <https://doi.org/10.1056/NEJM199710023371404>.
- [11] M. C. Thigpen, C. G. Whitney, N. E. Messonnier, E. R. Zell, et al. Bacterial meningitis in the united states, 1998–2007, *N. Engl. J. Med.* 364 (2011), 2016–2025. <https://doi.org/10.1056/NEJMoa1005384>.
- [12] B. Gleissner, M. C. Chamberlain, Neoplastic meningitis, *Lancet Neurol.* 5 (2006), 443–452.
- [13] K. Mann, M. A. Jackson, Meningitis, *Pediatr. Rev.* 29 (2008), 417–430.
- [14] V. J. Quagliarello, W. M. Scheld, Treatment of bacterial meningitis, *N. Engl. J. Med.* 336 (1997), 708–716.
- [15] S. Tartof, A. Cohn, F. Tarbangdo, M.H. Djingarey, et al. Identifying optimal vaccination strategies for serogroup a *neisseria meningitidis* conjugate vaccine in the african meningitis belt, *PLoS ONE* 8 (2013), e63605.
- [16] A. R. Tuite, D. N. Fisman, S. Mishra, Screen more or screen more often? using mathematical models to inform syphilis control strategies, *BMC Public Health* 13 (2013), 606.
- [17] J.-P. Chippaux, Control of meningococcal meningitis outbreaks in sub-saharan Africa, *J. Infect. Develop. Countries* 2 (2008), 335–345.
- [18] H. Ritchie, L. Rodés-Guirao, E. Mathieu, M. Gerber, E. Ortiz-Ospina, et al. Population Growth. <https://ourworldindata.org/population-growth>.
- [19] P. Van Den Driessche, J. Watmough, Further notes on the basic reproduction number, in: F. Brauer, P. Van Den Driessche, J. Wu (Eds.), *Mathematical Epidemiology*, Springer Berlin Heidelberg, Berlin, Heidelberg, 2008: pp. 159–178.
- [20] J. P. LaSalle, *The stability of dynamical systems*, SIAM, (1976).
- [21] Y. Zhou, B. Song, Z. Ma, The global stability analysis for an sis model with age and infection age structures, in: C. Castillo-Chavez, S. Blower, P. Van Den Driessche, D. Kirschner, A.-A. Yakubu (Eds.), *Mathematical Approaches for Emerging and Reemerging Infectious Diseases: Models, Methods, and Theory*, Springer New York, New York, NY, 2002: pp. 313–335.
- [22] E.X. DeJesus, C. Kaufman, Routh-hurwitz criterion in the examination of eigenvalues of a system of nonlinear ordinary differential equations, *Phys. Rev. A* 35 (1987), 5288–5290.
- [23] E. Bouza, M. G. De La Torre, F. Parras, A. Guerrero, M. Rodriguez-Creixems, J. Gobernado, Brucellar meningitis, *Clin. Infect. Dis.* 9 (1987), 810–822. <https://doi.org/10.1093/clinids/9.4.810>.

- [24] H. J. Kelley, R. E. Kopp, H. G. Moyer, 3 singular extremals, in: *Mathematics in Science and Engineering*, Elsevier, 1967: pp. 63–101.
- [25] W. H. Fleming, R. W. Rishel, G. I. Marchuk, et al. *Deterministic and Stochastic Optimal Control*, Springer, (1975).
- [26] R.E. Kopp, Pontryagin maximum principle, in: *Mathematics in Science and Engineering*, Elsevier, 1962: pp. 255–279.
- [27] G. T. Tilahun, Modeling co-dynamics of pneumonia and meningitis diseases, *Advances in Difference Equations* 2019 (2019), 149.
- [28] T. Koutangni, P. Crépey, M. Woringer, S. Porgho, B.W. Bicaba, H. Tall, J.E. Mueller, Compartmental models for seasonal hyperendemic bacterial meningitis in the African meningitis belt, *Epidemiol. Infect.* 147 (2019), e14. <https://doi.org/10.1017/S0950268818002625>.
- [29] S. Nana-Kyere, E. Okyere, J. De-Graft Ankamah, Compartmental SEIRW COVID-19 optimal control model, *Comm. Math. Biol. Neurosci.* 2020 (2020), 87.
- [30] M. I. Ossaiugbo, N. I. Okposo, Mathematical modeling and analysis of pneumonia infection dynamics, *Sci. World J.* 16 (2021), 73–80.
- [31] M. Martcheva, G. Crispino-O’Connell, The transmission of meningococcal infection: a mathematical study, *J. Math. Anal. Appl.* 283 (2003), 251–275.
- [32] M. J. F. Martínez, E. G. Merino, E. G. Sánchez, J. E. G. Sánchez, A. M. D. Rey, G. R. Sánchez, A mathematical model to study the meningococcal meningitis, *Proc. Comp. Sci.* 18 (2013), 2492–2495.
- [33] W. M. Ritha, W. Lily, Risk factors of meningitis in adults—an analysis using fuzzy cognitive map with TOPSIS, *Int. J. Sci. Innov. Math. Res.* 2 (2014), 418–425.
- [34] R. U. Hurit, S. Mungkasi, The Euler, Heun, and Fourth Order Runge–Kutta Solutions to SEIR Model for the Spread of Meningitis Disease. *Mathline* 6 (2021), 140–153.
- [35] B. Buonomo, A. d’Onofrio, S.M. Kassa, Y.H. Workineh, Modeling the effects of information-dependent vaccination behavior on meningitis transmission, *Math. Meth. Appl. Sci.* 45 (2022), 732–748.
- [36] C. W. Chukwu, J. Mushanyu, M. L. Juga, Fatmawati, A mathematical model for co-dynamics of listeriosis and bacterial meningitis diseases, *Comm. Math. Biol. Neurosci.* 2020 (2020), 83.
- [37] K. G. Varshney, Y. K. Dwivedi, Mathematical Modelling of Influenza–Meningitis under the Quarantine effect of influenza. *Turk. J. Comp. Math. Educ.* 12 (2021), 7214–7225.
- [38] M. A. Afolabi, K. S. Adewoye, A. I. Folorunso, M. A. Omoloye, A mathematical model on transmission dynamics of meningococcal meningitis, *Iconic Res. Eng. J.* 4 (2021), 59–66.
- [39] E. N. Wiah, I. A. Adetunde, A Mathematical Model of Cerebrospinal Meningitis Epidemic: A Case Study for Jirapa District, Ghana, *Curr. Appl. Sci. Technol.* 10 (2014), 63–73.
- [40] R. M. Neilan, S. M. Lenhart, An Introduction to Optimal Control with an Application in Disease Modeling, *Model. Parad. Anal. Dis. Trasmis. Models*, 49 (2010), 67–82.
- [41] I. M. Ross, *A Primer on Pontryagin’s Principle in Optimal Control*, Collegiate Publishers, (2009).
- [42] S. Lenhart, J. T. Workman, *Optimal control applied to biological models*, Taylor & Francis, (2007).
- [43] O. Sharomi, T. Malik, Optimal control in epidemiology. *Ann. Oper. Res.* 251 (2017), 55–71.
- [44] A.K. Misra, A. Sharma, J.B. Shukla, Modeling and analysis of effects of awareness programs by media on the spread of infectious diseases, *Math. Comp. Model.* 53 (2011), 1221–1228.
- [45] E. Bonyah, K. Badu, S.K. Asiedu-Addo, Optimal control application to an ebola model, *Asian Pac. J. Trop. Biomed.* 6 (2016), 283–289.
- [46] S. İğret Araz, Analysis of a covid-19 model: optimal control, stability and simulations, *Alex. Eng. J.* 60 (2021), 647–658.

- [47] X. Yan, Y. Zou, Optimal and sub-optimal quarantine and isolation control in SARS epidemics, *Math. Comp. Model.* 47 (2008), 235–245.
- [48] A. Karachaliou, A. J. K. Conlan, M. P. Preziosi, C. L. Trotter, Modeling long-term vaccination strategies with menafrivac in the african meningitis belt, *Clin. Infect. Dis.* 61 (2015), S594–S600.